ISSN 2349-7750

INDO AMERICAN JOURNAL OF
PHARMACEUTICAL SCIENCES

Available online at: http://www.iajps.com *Research Article*

FORMULATION AND EVALUATION OF GASTRO-RETENTIVE DRUG DELIVERY SYSTEM (GRDDS) LOADED WITH AN AMORPHOUS SOLID DISPERSION OF CLINIDIPINE PREPARED BY HOT-MELT EXTRUSION METHOD.

Dr. Amit singh, N.Sandeepthi* Dr.L.Satyanarayana
Monad University,Hapur,Uttarpradesh,245101

Abstract:
Owing to its many inherent advantages, oral administration is the most preferable route of medicinal administrations, and thus has a prominent role in therapy. However, it is also known as an unpredictable and fluctuating treatment route, especially with regard to active pharmaceutical ingredients (APIs) that have poor solubility, slow dissolution, low intestinal permeability, and narrow absorption window. Frequent problems of oral drugs include fluctuating pharmacokinetics, low bioavailability, and poor treatment efficiency. Most of the encountered problems stem from the low solubility of APIs, as well as the physiological fluctuations. It is estimated that approximately 40% of marketed APIs have problem with dissolution, and the majority of drug candidates currently in development are poorly soluble, and their absorption sites limited to the upper small intestine. Therefore, ensuring that drugs are completely dissolved and ready for absorption before passing through the small intestine is very crucial. To date, solid dispersion (SD) is one of the most successful strategies that enhances the dissolution and/or solubility of poorly soluble APIs. More advanced than conventional SD, amorphous SD can significantly enhance the apparent solubility, and therefore create a supersaturated solution in a non-sink condition. This ultimately raises the in situ *drug concentration at the absorption site, and thus is potential to enhance the drug absorption.*

Key words: *API, absorption window, bioavailability, solid dispersions.*

Corresponding author:
N.Sandeepthi,
Monad University,Hapur,
Uttarpradesh,245101

Please cite this article in press as N.Sandeepthi et al. ***Formulation and Evaluation of Gastro-Retentive Drug Delivery System (GRDDS) Loaded With An Amorphous Solid Dispersion Of Clinidipine Prepared By Hot-Melt Extrusion Method.,*** *Indo American J of Pharm Sci 2015:2(1):548-551.*

1.INTRODUCTION:

The gastrointestinal (GI) tract comprises many segments that are starkly different in both anatomy and internal environment, which crucially influences the *in vivo* dissolution and absorption of drugs. Ideally, drugs are completely dissolved and absorbed before they reach the colon, as small intestine is the main absorptive region with surface area approximately 120 times higher than the total area of all other parts of the GI tract [16]. However, the drug's retention time largely fluctuates depending on meals, dosage forms, and inter- and intra-subjective variations[11,24]. The gastric retention time may vary from several minutes to 3 h in the fasted state and from 1 to 10 h in the fed state. Meanwhile, the intestinal transition time, which is believed to be less variable, can be as short as 1 h or as long as 7 h, or even longer [28]. This ultimately results in large pharmacokinetic fluctuations and unpredictable treatment efficacy. Residing dosage forms in the stomach is a potential approach overcoming these drawbacks.

A gastro-retentive drug delivery system (DDS) can facilitate a more predictable release and allow for more complete absorption. Because *in vivo* dissolution is limited in the stomach, drug release tends to be more controlled [21]. Furthermore, drug concentration surrounding the dosage forms is maintained low, since the dissolved drug is continuously transported away from them, downward the intestine. This is very important with regard to low solubility drugs, as a pseudo-sink condition is created and *in situ* re-crystallization is prevented. In addition, drugs gradually enter the absorption site as free molecules ready for absorption which is practically meaningful to drugs with narrow absorption window and unpredictable bioavailability [20]. Finally, such a formulation maximizes the absorption area as the whole GI tract surface for all drug molecules. Since the drugs always release at the first segment, they all have the potential to be absorbed at any point throughout the tract. In contrast, for conventional DDSs, absorption area decreases significantly along with their downward movement. Therefore, taken as a whole, the gastro-retentive amorphous SD is a viable solution to the pharmacologic problems of narrow absorption window, low solubility, and poor absorbability.

The short gastric retention time of conventional dosage forms might limit the advantages of controlled-release DDSs, which usually prolong drug, release up to 12 h or longer. It is estimated that the average drug retention time in the stomach is around 30 min [11], and in the small intestine it is around 3 h [13]. This indicates that conventional controlled-release dosage forms might pass through the small intestine, the main absorption site, in 1/4 to 1/3 of their life spans, resulting in incomplete drug absorption. Therefore, they might only be suitable for APIs that can be absorbed well in the colon. Otherwise, the gastro-retentive DDS is a viable approach to the controlled release drugs.

There are numerous approaches to the fabrication of a gastro-retentive dosage form, including floating DDSs, sinking DDSs, expanding DDSs, bio-adhering DDS, and magnetic DDSs[8]. Among those, floating and bio-adhesive DDSs are the most extensively researched as well as developed as marketed products[12]. However, the floating DDS can be dislodged by the gastric emptying in an average of every 2 h [19], while the bio-adhesive DDS can be detached from the stomach wall by the mucus turnover that frequently renews the gastric mucosa outer layer[2]. The combination of the floating and bio-adhesive approaches, however, could potentially result in a synergistic effect that could effectively resist the stomach's physiological activities to maintain gastric retention for a suitable period of time.

Hot-melt extrusion (HME) is widely known as a green processing technology in the SD development in which APIs are dispersed and stabilized in polymer and lipid matrixes [15,17]. It is an excellent alternative to conventional techniques in the production of SDs [14]. With the application of the process analytical technology, PAT strategy, it can be systematically scaled up and developed as a continuous process [23,27,5]. To enhance applicability, in the present study, we developed a novel dual-mechanism gastro-retentive DDS loaded with amorphous SD of a BCS class II drug by utilizing a single step of HME. The prepared DDS can potentially resist the gastric dislodgement *via* the synergistic effect of floatation and bio-adhesion. It also can generate and maintain *in situ* drug super saturation, a viable solution to the problem of poor bioavailability.

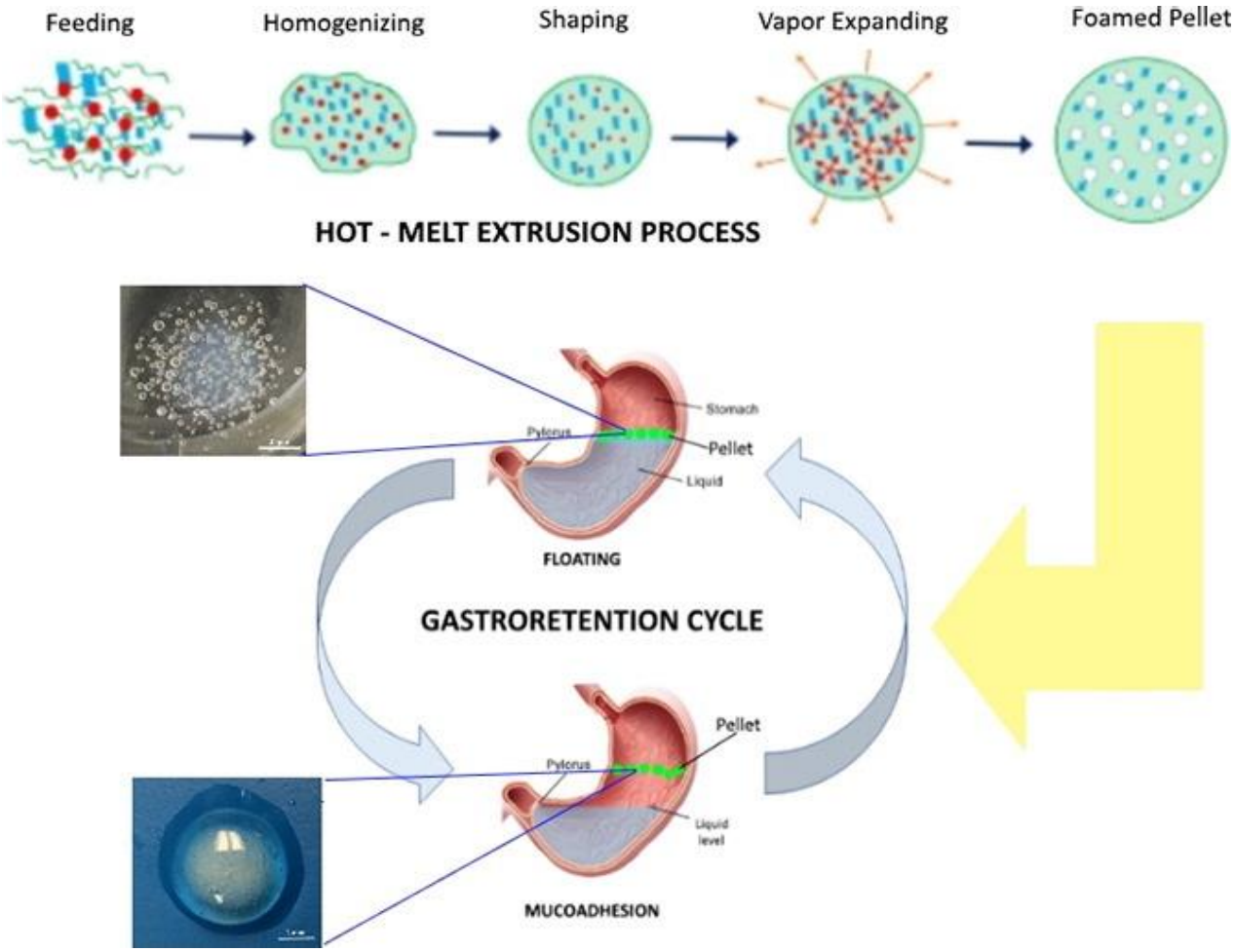

Figure 1: Graphical representation of Hot-melt extrusion and Gastro-retentive cycle

2. EXPERIMENTAL:

2.1. Materials:

Clinidipine USP was bought from Ria International LLC (East Hanover, NJ, USA). Sodium bicarbonate (SBC) USP/NF was acquired from Spectrum Chemical Mfg. Corp. (Gardena, CA, USA). HPMC K15M (Benecel K15M) and HPC (Klucel MF) were compassionately given by Ashland, Inc. (Lexington, KY, USA). HPLC solvents and every single other reagent utilized as a part of the investigation were of diagnostic review and were acquired from Fisher Scientific (Pittsburgh, PA, USA).

2.2.Extrusion Processing:

At first, crude materials were independently gone through a USP #35 work sifter to evacuate totals and clusters. A blend of 100 g of every plan was readied and physically blended until the point when a homogenous physical blend was gotten.

The framework utilized for setting up the frothed strands was included a twin screw extruder (Process 11™, Thermo Fisher Scientific, Odessa, TX, USA) furnished with a 1.5 mm roundabout bite the dust embed, a chiller, a feeder, and a transport line that was acclimated to synchronize with the principle module. A changed screw design (Fig. 2) was utilized for the test. The temperature of each of the eight zones on the barrel and the pass on was set at 165 C. Screw speed and sustaining rate was set at a steady 200 rpm and 5 g/min, separately.

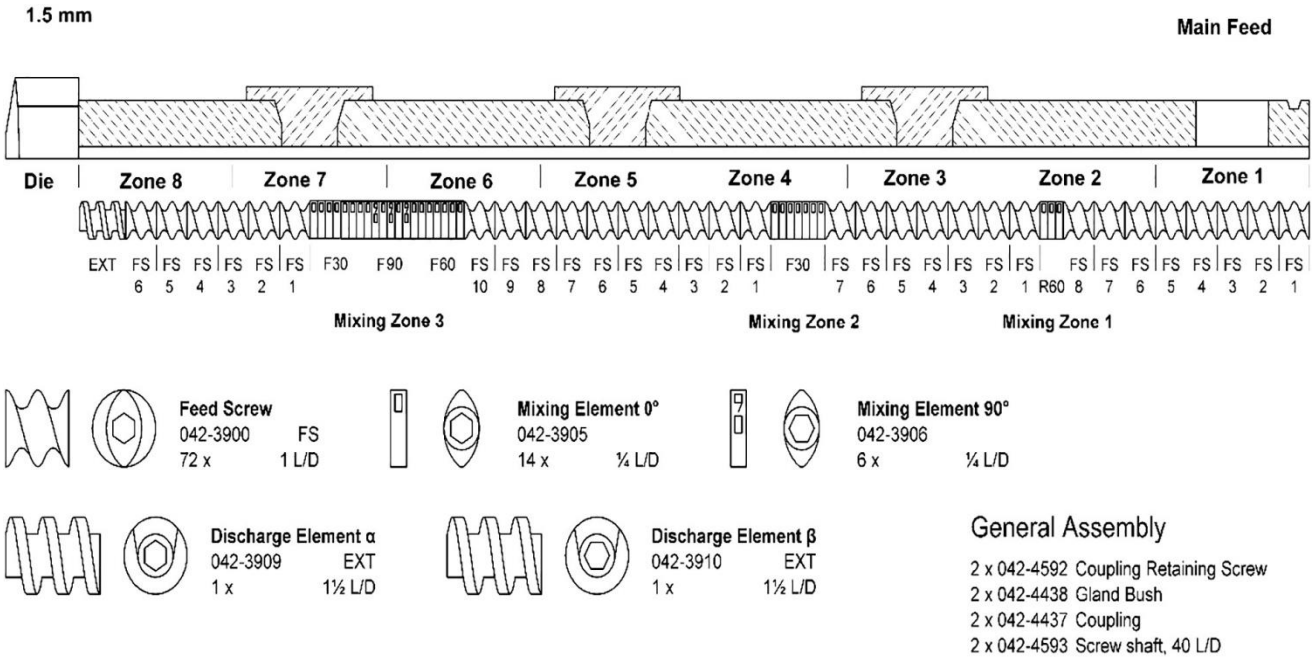

Fig.2: Modified screw configuration used to prepare the foamed pellets loaded with amorphous solid dispersion

The framework was permitted to warm splash for 10 min to build up warm balance before handling. The initial 30 g of the extrudate was disposed of to guarantee that the examples were gathered when the extruder was working at a relentless state. To get a consistently tube shaped extrudate, the transport speed was changed in accordance with synchronize with the extrudate arrangement rate. The straight extrudates were thusly cut into 2.0-mm long pellets and put away in tight glass bottles at 20– 25 °C.

2.3. Differential Scanning Calorimetry:

Differential Scanning Calorimetry (DSC) was utilized to explore the warm conduct of the materials and plans, and in addition to affirm the similarity of the API and the excipients. The unadulterated segments, their parallel blends (1:1), physical blends, and details were subjected to DSC experimentation (Diamond DSC Perkin Elmer, Waltham, MA, USA). Tests measuring 2– 5 mg (for unadulterated mixes) or 8– 12 mg (for physical blends) were stacked onto a pleated aluminum skillet (non-hermetic container) and put in the DSC framework. The examples were then balanced out by holding at a temperature of 45 °C for 2 min and took after by warming from 45 °C to 200 °C at a slope rate of 10 °C/min under an inactive nitrogen stream of 20 mL/min. The thermograms were examined to identify for warm occasions.

2.4.Experimental Design:

A two-level full factorial outline was connected to address the impacts of detailing pieces on pellet qualities. By utilizing this model, huge info components and connections between variables can

be recognized. Besides, the impacts of info variables can be scientifically portrayed and results can be anticipated for each set estimation of information factors. The consequences of the relapse are extremely valuable for outlining operation spaces in the quality by plan (QBD) approach.

The regression equation is expressed as follows:

$$Y_i = b_i + a_{i1}X_1 + a_{i2}X_2 + a_{i3}X_3 + a_{i12}X_1X_2 + a_{i13}X_1X_3 + +a_{i23}X_2X_3$$

Where Yi is the reaction number i, bi is the consistent, and ai1, ai2, ai3, ai12, ai13, ai23are the coefficients of the encoded factors. The hugeness of the model and impact of variables decided the relapse and one-route examination of difference (ANOVA) performed on Modde 8.0 programming (Umetrics Inc., Sweden). Three free factors were researched: Drug stack, HPMC substance, and SCB rate. The yield factors were tranquilize discharge profiles, porosity, and coasting qualities.

2.5. Scanning Electron Microscopy

The pellets were precisely sliced to deliver level surfaces for SEM examination. The examples were stuck on aluminum stubs held with a twofold sided carbon cement film and put in the covering chamber. The covering was performed in an idle gas condition arranged by expelling the air at 40 mm Hg, at that point filling the chamber with high virtue nitrogen. The specimens were then covered with gold by utilizing a Hummer® 6.2 Sputtering System

(Anatech LTD., Battlecreek, MI, USA) in nitrogen condition at 120 mm Hg and current of 18 mA. The covering was triplicated for 45 s each. The pellets' surface geology was analyzed utilizing a checking electron magnifying lens (SEM) working at a quickening voltage of 5 kV and an amplification of 45 × (JEOL JSM-5600; JEOL, Inc., Peabody, MA, USA).

2.6. X-Ray Diffraction

The X-Ray diffraction tests were performed by utilizing a Rigaku X-beam hardware (D/MAX-2500PC, Rigaku Corporation, Tokyo, Japan) with a copper tube anode and a standard example holder. The diffractograms were gathered at room temperature (20– 25 °C) with the accompanying parameters: step width of 0.02°/s, checking range from 5° to 40° on a 2θ scale; generator strain (voltage) 40 kV; generator current 100 mA; examining speed 10°/min.

2.7. Densities and Porosity:

To quantify geometric thickness, uniform straight strands were cut into 10-cm barrels with level surfaces on the two sides. The breadth (d), a normal of 5 unique estimations along the length of the barrel, and length (h) of the chambers were measured utilizing computerized calipers (d = 0.01 mm, VWR Digital Caliper, Radnor, PA, USA). The barrels were measured (m) utilizing a high exactness adjust (Analytical Balance XSE 204, Mettler Toledo, Switzerland). The pellet geometric thickness was ascertained utilizing the accompanying condition:

$$D_{\text{geometric}} = \frac{4m}{hd^2}$$

The pellet genuine thickness was resolved utilizing a gas pycnometer (AccuPyc II 1340, Micrimeritics, Norcross, GA, USA) utilizing helium gas. The estimations were imitated five times and the information were prepared utilizing the worked in programming suite. The outcomes mirrored the thickness of the framework skeleton, as the helium gas possessed the sum of the vacuous space inside the grid. The porosity of the gliding pellets was computed utilizing the accompanying condition:

$$P = \frac{V_{void}}{V_{geometric}} = 1 - \frac{D_{geometric}}{D_{skeletal}}$$

where Vvoid is the aggregate volume of the air pockets inside the pellets, and Vgeometric is the volume of the pellet all in all protest. Dgeometric and Dskeletal are the geometric thickness and genuine thickness of the pellets, individually.

2.8. Sample Process for Quantitative Analysis

Utilizing a mortar and pestle, the extrudate was ground into a fine powder. It was then precisely weighed to a sum proportional to 10 mg of CLINIDIPINE and moved into a 100-mL volumetric jar alongside 40 mL acetonitrile and 20 mL methanol. The flagon was sonicated for 5 min (Branson 2510, Branson Ultrasonic Corp., Danbury, CT, USA) before including 30 mL phosphate cradle (pH = 3) and consistently shaken for 15 min utilizing a mechanical shaker. The cradle was added to the volume and blended well. A volume of 5 mL was centrifuged at the relative rotator power of 16,000 g for 10 min at 25 °C (Centrifuge 5415R, Eppendorf AG, Eppendorf, Germany). The supernatant was weakened five times with the versatile stage and sifted with a 0.45-µm film before stacking into the auto-sampler of the superior fluid chromatography i.e. HPLC system.

2.9. HPLC Analysis

Clinidipine was analysed using a Waters 600 HPLC system (Waters Corp., Milford, MA, USA) equipped with an auto-sampler, UV/VIS detector, and a Phenomenex® Luna C18 column (5 µm, 250 mm × 4.6 mm). The HPLC program was developed after referencing the USP Clinidipine extended release tablet monograph. The mobile phase was a mixture of acetonitrile: methanol: Potassium dihydrogen phosphate buffer (6.9 g mono basic KH_2PO_4 in a 1000 mL solution, adjusted with ortho-phosphoric acid to pH 3) at a ratio of 3:2:1 (v/v). The elution was performed at a flow rate of 1.0 mL/min in an isocratic mode. The injection volume was set at 10 µL for the assay samples, and 50 µL for the dissolution samples. The signal was detected at a wavelength of 365 nm. Two linear calibration curves were established, one ranging from 0.4375 µg/mL to 28 µg/mL (R^2 = 0.9998), which was used to analyse the assay samples and dissolution in sink condition samples. The other ranged from 0.0252 µg/mL to 3.220 µg/mL (R^2 = 0.9983), which was used to quantify the dissolution in fasted state simulated gastric fluid (FaSSGF) samples.

2.10. *In Vitro* Drug Release

Floating pellets (10 mg CLINIDIPINE) were subjected to dissolution testing in a sink condition and biorelevant dissolution medium. The sink condition dissolution medium consisted of 900 mL 1% SLS in 0.1 N HCl solution. The un-sink

dissolution media was the FaSSGF whose composition was described by Marques et al. (2011) and Jantratid et al. (2008). The paddle method and USP dissolution apparatus type 2 (Hanson SR8; Hanson Research, Chatsworth, CA, USA) were used with a setting temperature of 37 ± 0.5 °C and paddle rotation speed of 100 rpm. At predetermined time points, a volume of 2.0 mL dissolution media was withdrawn and 2.0 mL fresh dissolution media was added. The samples were subsequently filtered through 0.2 µm, 13 mm PTFE membrane filters (Whatman, Inc., Haverhill, MA, USA). Samples of the dissolution test in biorelevant media were diluted with an equal volume of an acetonitrile: methanol (2:1) mixture before injection into the HPLC system. A volume of 10 µL (assay test) or 50 µL (dissolution test) was injected into the HPLC system for analysis by the above method.

3. RESULT AND DISCUSSION

In the present study, we first aimed to fabricate a hydrophilic matrix because the model drug was a poorly soluble compound, and we hypothesized that such a matrix would help enhance drug dissolution. HPMC is the most important hydrophilic polymer in the formulation of controlled-release DDSs. It can swell to form an erodible hydrogel that controls drug release from the matrix (Siepmann and Peppas, 2001). In addition, HPMC is an excellent carrier for amorphous drugs owing to its high Tg (> 180 °C) and ability to maintain the super-saturation of drugs in aqueous media (Konno et al., 2008); (Yang et al., 2015). However, it is not a good candidate for HME because HME generates high pressure, high torque, and requires a high processing temperature that is close to HPMC's degradation temperature. Thus, HPC was chosen as the secondary polymer to enable the HME process because it has a chemical structure very similar to that of HPMC; thus, it is potentially able to be melt-miscible with HPMC. Furthermore, its low Tg can be used to modulate the Tg of the polymer blend according to the Gordon-Taylor equation (Forster et al., 2001).

The foamed strands were formed as the extrudate exited the die based on the expansion of CO_2 generated from thermal degradation of $NaHCO_3$. We hypothesised that the processing temperature would be higher than the degradation temperature of the foaming agent, but simultaneously low enough to ensure the stability of formulations during processing. The optimum processing temperature was chosen based on the DSC experimental results as shown in Fig. 3. The degradation process reached its peak at approximately 150 °C and finished below 170 °C. Therefore, the processing temperature was chosen to be 165 °C, the lowest temperature where the foaming effect of SBC could be maximized. This temperature was also higher than the melting temperature of the API, facilitating API dispersion into the polymer matrix.

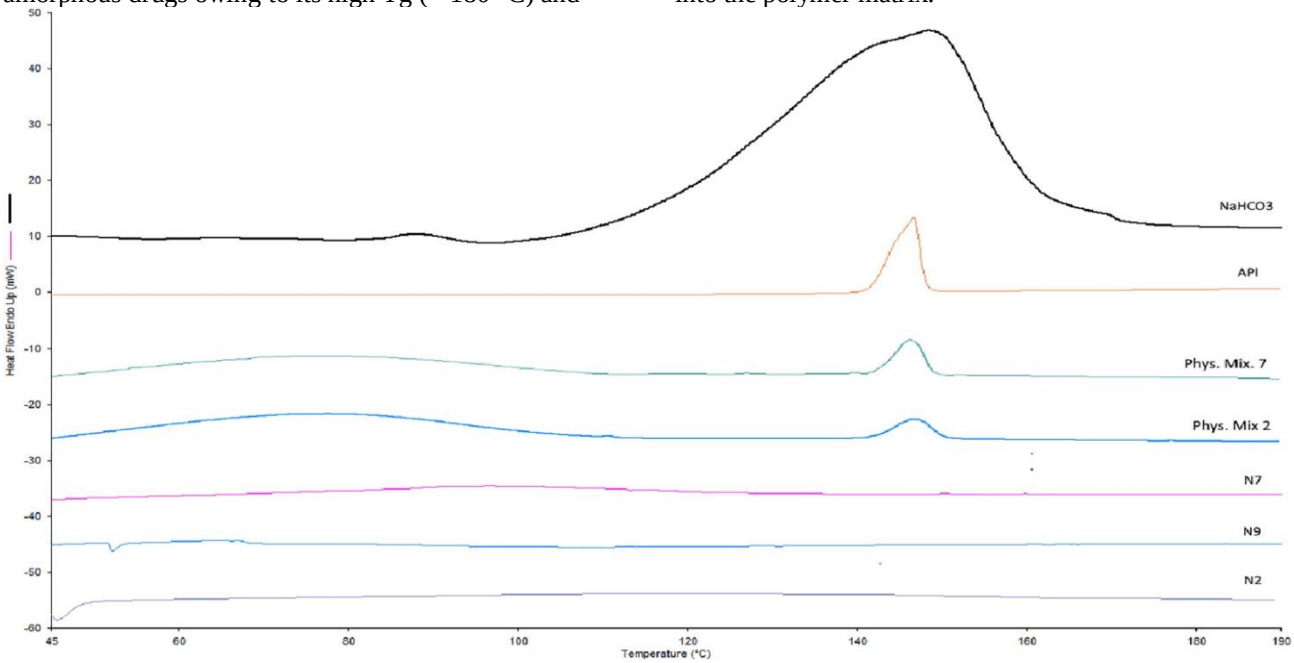

Fig.3: Thermogram of API, foamed agent, selective formulations, and selective physical mixtures in which sodium bicarbonate was substituted by sodium carbonate (drug load in physical mixture 2 was 6%; and Phys. Mix. 7 was 14%).

A series of preliminary experimentations were conducted to determine the parameters for experimental feasibility. The screw configuration was redesigned as shown in the Fig. 2 to enhance the performance of the foamed extrusion process. A small reverse mixing zone was set at the second barrel zone to create a temporary melting seal to prevent gas leakage. In addition, all three mixing zones were moved forward towards the barrel end, and the first two mixing zones were simplified to enable the materials to be conveyed into the tight area more quickly. To compensate the first two small mixing zones, the last mixing zone was increased in size and designed more complexly to ensure a good homogeneity effect. The feeding rate was fixed at 5 g/min and screw speed was set at 200 rpm to satisfy various requirements, such as the ability to fill the barrel, to synchronize with the strand conveyance, and to generate a suitable foamed strand.

The design of experiment (DOE) was used to elucidate the effects of formulations on the properties of the pellets. The HPMC content, drug load, and SBC percentage were chosen as independent factors with their variable ranges shown in Table 1. HPC was considered a compensated variable. From the preliminary study, the variation range of HPMC content ranged from 25% to 35%. If it was higher than 40% the torque would increase and the extrudate would be too hard that did not allow for the formation of foamed strands (Fig. 4B); if it was lower than 25%, the extrudate was too soft, and the strands would burst and ultimately shrink, such that the foam structure could not be maintained (Fig. 4A). The SBC range of 5–9% was chosen such that a suitable foamed structure could be obtained. If the SBC was out of the range, either the pellets would have too low porosity to enable them float, or they would be too porous to be effective. The drug load varied around 10%, based on the presumption that the drug and polymers would be completely miscible and physically stable.

Table 1: Experimental independent factors and their variation.

Independent variable	Symbol	Unit	Coded value		Real value	
			Upper	Lower	Upper	Lower
HPMC content	X1	%	+ 1	− 1	36	24
Drug load	X2	%	+ 1	− 1	15	5
SBC percentage	X3	%	+ 1	− 1	10	4

HPMC: Hypromellose; SBC: Sodium bicarbonate.

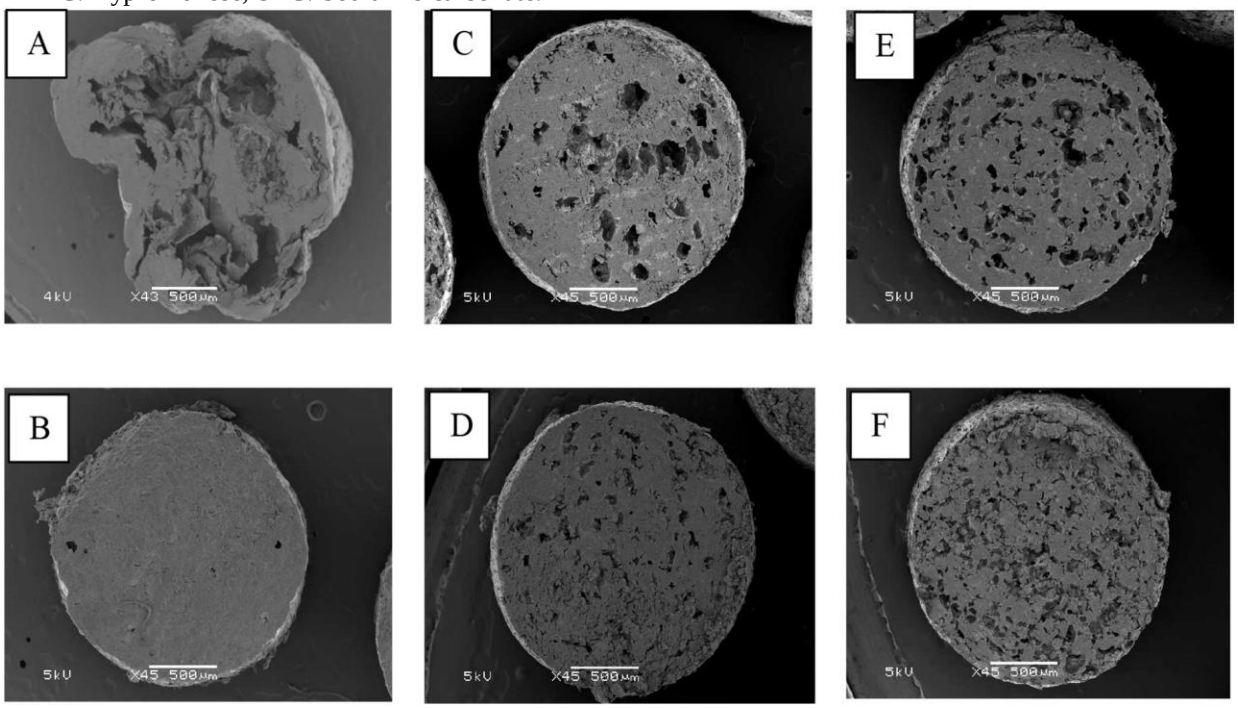

Fig. 4:Representative scanning electron microscope (SEM) images of the pellets' cross-sectional surface. (A) 0% HPMC; (B) 50% HPMC; (C) 25% HPMC and 5% SBC-N1; (D) 35% HPMC and 5% SBC-N2; (E) 25% HPMC and 9% SBC-N7; (F) 35% HPMC and 9% SBC-N8.

Table 2: Experimental formulation compositions.

Formulation	Run order	X1	X2	X3	HPC (%)
N1	11	25	6	5	64.5
N2	8	35	6	5	54.5
N3	9	25	14	5	55.5
N4	4	35	14	5	45.5
N5	10	25	6	9	60
N6	3	35	6	9	51
N7	6	25	14	9	52
N8	7	35	14	9	42
N9	5	30	10	7	54
N10	2	30	10	7	54
N11	1	30	10	7	54

All 11 DOE formulations were successfully prepared. Within the experimental ranges, the system worked smoothly and uniformly foamed strands were obtained. When a steady state was established, the torque and die pressure remained relatively stable around 2.5 Nm (25%) and 26 bars, respectively. Even though the operation temperature was lower than the Tg of HPMC, the torque was quite low because HPMC was miscible with the softened HPC and was able to form a polymer blend with lower Tg. In addition, it is possible that the melted CLINIDIPINE plasticized and/or produced a lubricant effect that further decreased the torque. The total retention time of the formulations in the barrel and die was approximately 80 s.

3.1. Micromeritics Properties:

Eleven DOE formulations (Table 2) were fabricated and characterized. The SEM images of the pellets' cross-sectional surfaces revealed vacant spaces inside the pellets created by the expanded CO_2 in all 11 formulations. The size and distribution of vacant spaces depended on the HPMC content and SBC percentage. Generally, the SBC percentage had a covariant effect on the size and degree of vacant spaces, and HPMC content had a contra variant effect, as shown in Fig. 4.

The micromeritics properties of the pellets are presented in Table 3. The density of all 11 formulations was lower than 1 g/cm^3, allowing them to immediately float on top of the gastric fluid (Fig. 5), additionally confirming their foamed structure. The extrudate drug load ranged from 97.70–100.16% compared to theoretical values, which implies that the drug was stable during processing. The loss on drying (105 °C for 15 min) of the samples was considerably low (1.18–1.86%) compared to their respective physical mixtures. Under the high processing temperature, most of water evaporated once the extrudate exited the die. Since water would largely effect on molecular mobility *via* decreasing the Tg of SD, low water content would significantly increase the physical stability of an amorphous SD.

Because the pellet true density (or skeletal density) of all 11 formulations was almost the same, the pellet porosity was proportional related to the pellet geometry density. Hence, the porosity proportionally reflected the initial floatability of the pellets, which could not be measured because of large fluctuations. The regression result confirmed that the model used was suitable for describing the relationship of the input factors to pellet porosity ($R^2 = 0.987$, $Q^2 = 0.751$). While drug load did not significantly affect pellet porosity, both the HPMC content and SBC percentage had significant effects ($P < 0.01$). The SBC percentage positively affected pellet porosity, as it controlled the amount of temporary blowing agent generated.

In contrast, HPMC content inversely affected pellet porosity. It moderated the softening of the hot polymer matrix, and thus matrix expansion. Its high Tg also helped to preserve the foa8med structure by quickly hardening the extrudate when it exited the die. However, the SBC percentage effect was three times higher than that of HPMC content.

Previously, there were a few published studies on floating dosage forms prepared using HME. Those studies focused on highly soluble compounds, used Eudragit RS as a matrix forming polymer, and owed high risk of dislodgement by gastric emptying. In one study, floating tablets were prepared based on the expansion of CO_2 generated from the reaction of SBC and acetohydroxamic acid (Fukuda et al., 2006); however, the continuous reaction of the residual acid and base during storage is problematic for stability.

Recently, gas-generated floating particulates, whose buoyancy depended on gastric pH, were prepared using HME (Malode et al., 2015). However, this process is possibly unpractical for product development because of extremely low throughput and long resident time inside the barrel (9 min). In comparison to the other floating dosage forms, the particulate buoyancy was limited because the lag time (> 3 min); after 5.5 h and 10.5 h, > 50% and 90% of the particulates sank, respectively. More recently, floating foamed pellets were prepared by injecting an inert foaming agent into the extruder barrel (Vo et al., 2016). The obtained pellets showed good floating kinetics with no lag time, with floating time > 12 h and floating force as high as 5000 μN/g.

3.2. Thermal Properties:

The thermal behavior of materials and formulations were elucidated using DSC. From the results shown in Fig. 3, no thermal event was detected in the range of 40–190 °C on the thermogram for HPC and HPMC that could confirm the amorphous nature of these two polymers. An exothermic peak at 146 °C corresponded to the melting peak of the crystalline Clinidipine raw material. On the thermogram for SBC, a large, broad exothermal event that noticeably started at 110 °C could be interpreted as a thermal degradation peak.

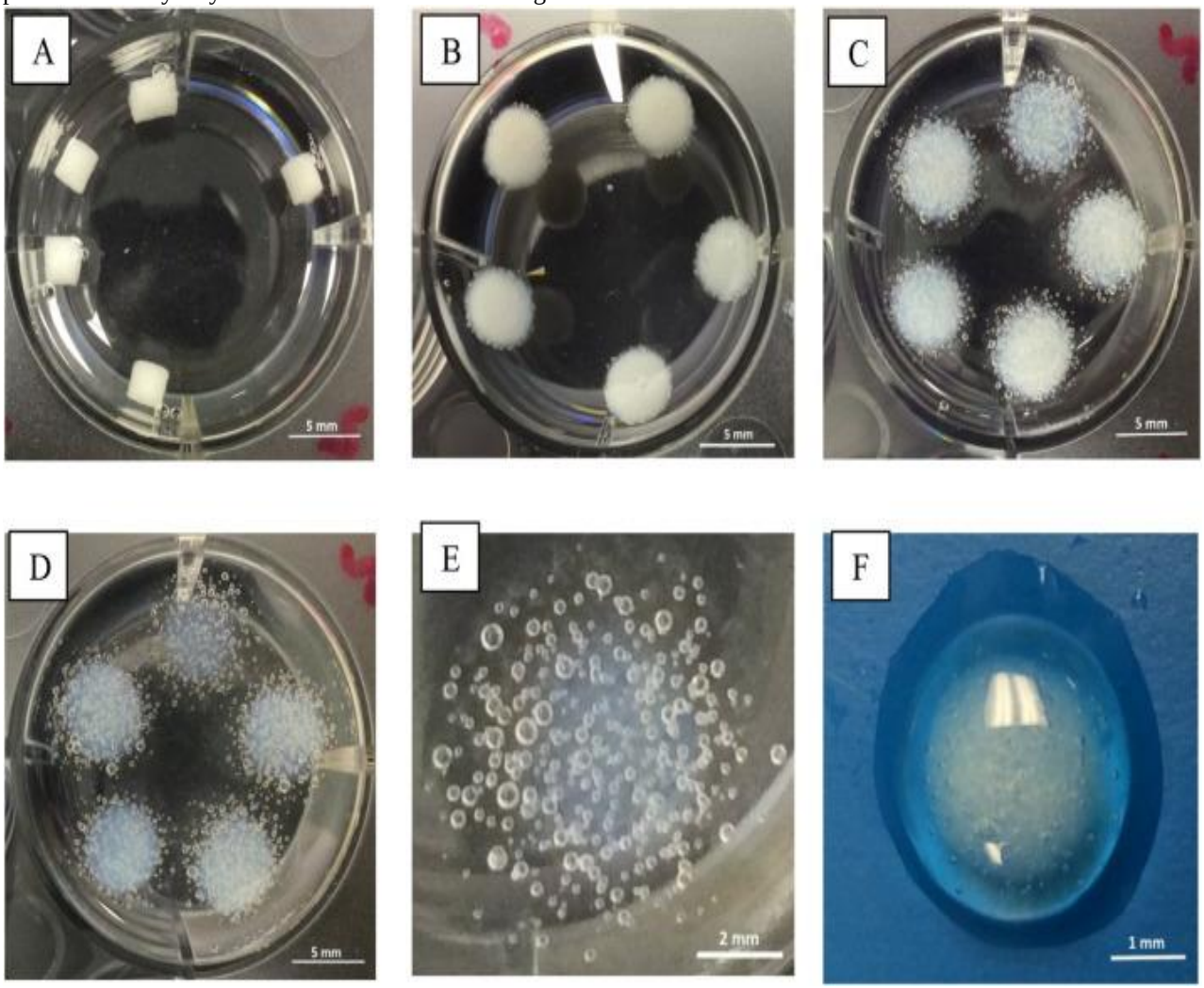

Fig. 5. Appearance of the pellets in dissolution medium. (A) Initial. (B) 1 h. (C) 4 h. (D) 8 h. (E) 12 h. (F) Formation of the gel layer after 1 h.

CO_2 and H_2O generated from the SBC degradation reaction could evaporate and remove heat from the DSC sample, thus causing the heat to flow to the sample to compensate for the heat lost, resulting in the exothermic peak. There was no detectable thermal event in the thermograms of all 11 formulations. This further suggests that the crystalline Clinidipine was transformed into an amorphous form, and the SBC in the starting formulations had maximized its effect. The amorphous form of Clinidipine in the formulations was confirmed by XRD results. The sharp peaks in the region of 23^o to 26^o that presented in pure Clinidipine and the low drug load physical mixture could not be detected in the diffractogram of formulations with both low and high drug load (Fig. 6).

Table 3: Micromeritic properties of the foamed pellets (± SD).

Form.	Geometric density (g/cm^3)[a]	True density (g/cm^3)[b]	Porosity (%)	Physical mixture LOD (%)	Pellet LOD (%)	Drug load (%)[a]
N1	0.9201	1.3004	29.25	4.51	1.82	6.05
	± 0.0169	± 0.0004				± 0.121
N2	0.9761	1.2834	24.57	4.78	1.88	6.06
	± 0.0212	± 0.0002				± 0.01
N3	0.9171	1.2678	28.98	4.35	1.61	14.82
	± 0.0199	± 0.0004				± 0.19
N4	0.9572	1.2919	26.01	4.64	1.49	14.97
	± 0.0202	± 0.0002				± 0.19
N5	0.7661	1.2931	40.82	4.75	1.50	6.62
	± 0.0190	± 0.0006				± 0.05
N6	0.8411	1.2929	34.92	4.68	1.47	6.51
	± 0.01799	± 0.0002				± 0.62
N7	0.7880	1.2869	39.12	4..14	1.24	14.65
	± 0.01912	± 0.0004				± 0.25
N8	0.8331	1.2948	35.66	4.85	1.20	14.94
	± 0.0259	± 0.0003				± 0.17
N9	0.8711	1.2901	32.92	4.47	1.39	10.13
	± 0.0182	± 0.0003				± 0.18
N10	0.8731	1.2941	32.58	4.59	1.46	10.31
	± 0.0061	± 0.0003				± 0.06
N11	0.8812	1.2888	31.82	4.41	1.41	10.42
	± 0.0141	± 0.0002				± 0.07

LOD: Loss on drying. a $n = 3$. b $n = 5$.

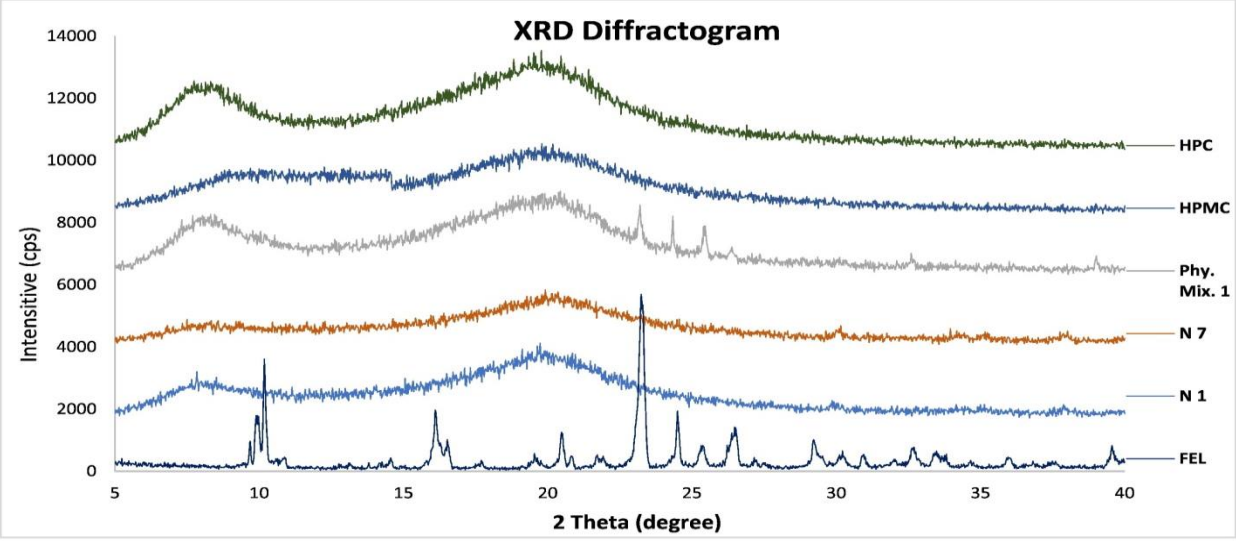

Fig.6: XRD diffractogram of crystal Clinidipine, polymers, low drug load physical mixture, and selective

formulations with low and high drug load.

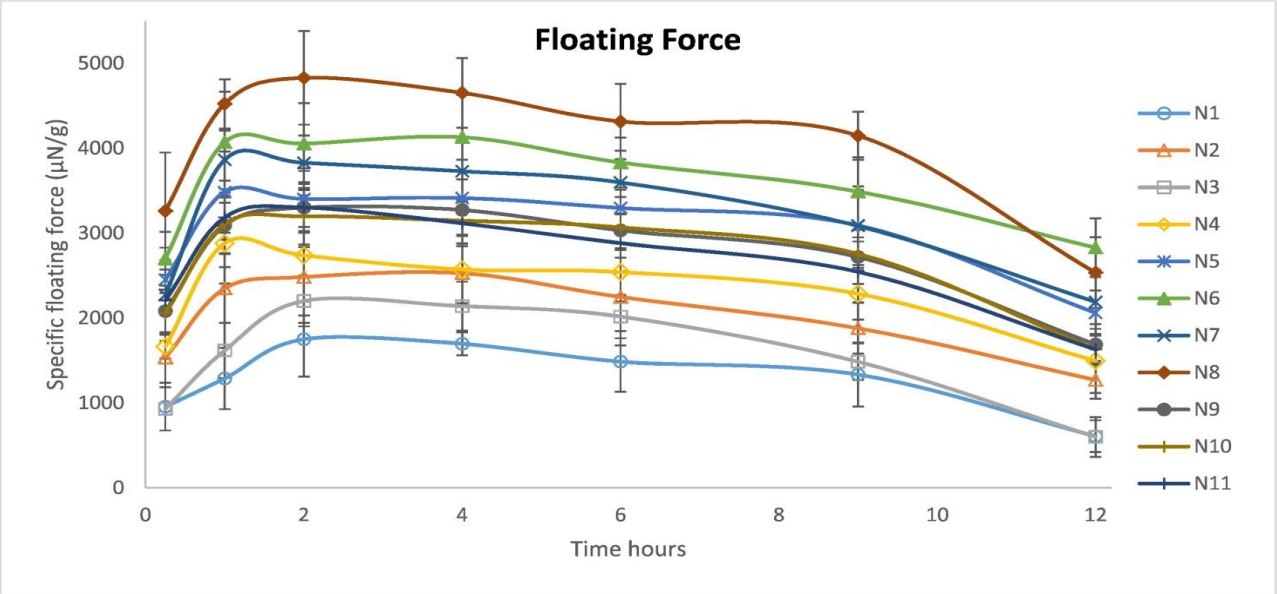

Fig. 7: Specific floating kinetics of the pellets (± SD, *n* = 3).

3.3. Floating Kinetics

A floating dosage form might experience many obstacles that prevent it from maintaining buoyancy for a sufficient period of time. Floating force is the most crucial parameter in evaluating buoyancy, as it shows how well a dosage form can float (Timmermans and Moes, 1990). High floating force enables the dosage form to resist submergence and assists it in refloating when the submergence might temporarily occur.

Owing to their low density ($d < 1.00$), all 11 formulations could float immediately on top of FaSSGF. Upon contact with the gastric fluid, the polymers rapidly absorbed water and swelled, with a gel layer forming to cover the matrix, trapped bubbles, and maintain floatation for over 12 h (Fig. 5). To investigate the floating kinetics, the buoyant force of the pellets in FaSSGF was measured at different time points over 12 h. The floating kinetics greatly varied from one formulation to the other (Fig. 7). The initial floating force could not be measured accurately, as the simultaneous effects of the swelling process and the reaction of sodium carbonate (SC), which was formed from the thermal degradation of SBC and remained in the formulations, with acid from the environment caused the force to continually increase. The increase in the floating force in the first 60 min was proportionally related to the SBC percentage. Afterwards, it became relatively constant up to 9 h, before dropping off. During the first 9 h, the bubbles escaping from the matrix were compensated by the CO_2 generated from SC, ultimately keeping the floating force stable (Table 4). When the SC was exhausted, the loss of vacant space in the matrix overcame gas generation, that would make the floating force decrease at a rapid rate.

The regression results of the floating force at 1 h and 9 h (Table 5) confirmed that the model used could accurately describe the effects of input factors on output variables ($P < 0.05$, $R^2 > 0.98$, $Q^2 > 0.485 \approx 0.50$). The floating force was significantly ($P < 0.05$) governed by all three factors in a positive manner. Among the three factors, SBC percentage had the greatest effect on both probability and capability (Fig. 8). This effect on pellet floatability probably acted *via* two different mechanisms; on the one hand, it controls pellet porosity (Table 5), which is proportionally related to the initial floating force and the pellet's intrinsic floating ability. On the other hand, SC in the pellets would react with acid in the gastric fluid and generate CO_2, increasing the floating force. This would explain why the floating force remained relatively stable up to 9 h. As for the role of HPMC, its high viscosity contributed to gel layer density, retarded polymer dissolution, and thus trapped air bubbles in the matrix more effectively. The greater the HPMC content, the higher the floating force observed. FEL, a hydrophobic compound, influenced pellet floatability *via* its contribution to the hydrophobicity of the matrix, retarding water penetration into pellets and positively affecting the floating force. Drug load contributed the least to the pellet buoyancy. With regard to the floating force during the first hour, there

was no potential interaction (P > 0.58) between input factors, so the regression could be considered a linear regression. However, there was a potential interaction between HPMC content and drug load at 9 h (P = 0.056), which inferred a possibly significant effect of (drug load ∗ HPMC content) to floating force.

Table 4: Floating efficiency of the pellets.

Form.	Floating strength (μN/g)			
	1 h		9 h	
	Average	SD	Average	SD
F1	1291	361	1334	376
F2	2351	407	1880	298
F3	1621	328	1486	214
F4	2879	476	2287	305
F5	3486	478	3093	416
F6	4071	594	3491	404
F7	3869	345	3086	464
F8	4521	290	4148	284
F9	3099	327	2719	319
F10	3111	510	2756	194
F11	3191	261	2545	358

Table 5. Floating efficiency regression result.

Variables	Pellet porosity		Floating force at 1 h		Floating force at 9 h	
	Coefficient	P	Coefficient	P	Coefficient	P
Model		0.001		0.001		0.002
Constant	0.3227	0.000	3043.1	0.000	2620.5	0.000
X1	− 0.0170	0.008	371.0	0.004	306.7	0.003
X2	− 0.0030	0.401	225.02	0.022	158.4	0.021
X3	0.0462	0.001	877.1	0.000	761.01	0.000
X1 ∗ X2	0.0039	0.252	28.2	0.637	97.41	0.051
X1 ∗ X3	− 0.0056	0.119	− 26.6	0.660	1.77	0.961
X2 ∗ X3	− 0.0016	0.611	− 32.4	0.583	18.1	0.649
	R^2 = 0.984 Q^2 = 0.736		R^2 = 0.982 Q^2 = 0.492		R^2 = 0.992 Q^2 = 0.565	

R^2, goodness of fit; Q^2, goodness of prediction.

3.4. Bio-adhesive Properties

Upon contact with gastric fluid, the pellets would absorb water and swell to produce a highly viscous and sticky hydrogel outer layer. The high viscosity enabled the pellets to initially adhere to the stomach wall. In addition, the HPC and HPMC polymer chains might penetrate into the mucus layer and interlock with the glycoproteins of the mucosa (Varum et al., 2010). Furthermore, upon contact with the stomach mucosa, hydrogen bonding between ⎯OR (R = hydrogen or a short chain hydrocarbon) groups of the polymer and ⎯NH_2 and ⎯COOH groups of the mucosa protein occur (Andrews et al., 2009), further increasing the bio-adhesion force of the pellets. Because both HPMC and HPC are rich in ⎯OR groups, the generated hydrogen bonds significantly contribute to the bio-adhesion force. The total adhesion force was thus expected to be high enough to keep the pellets attached to the stomach wall during the gastric emptying process, which occurs periodically as a physiological activity of the stomach.

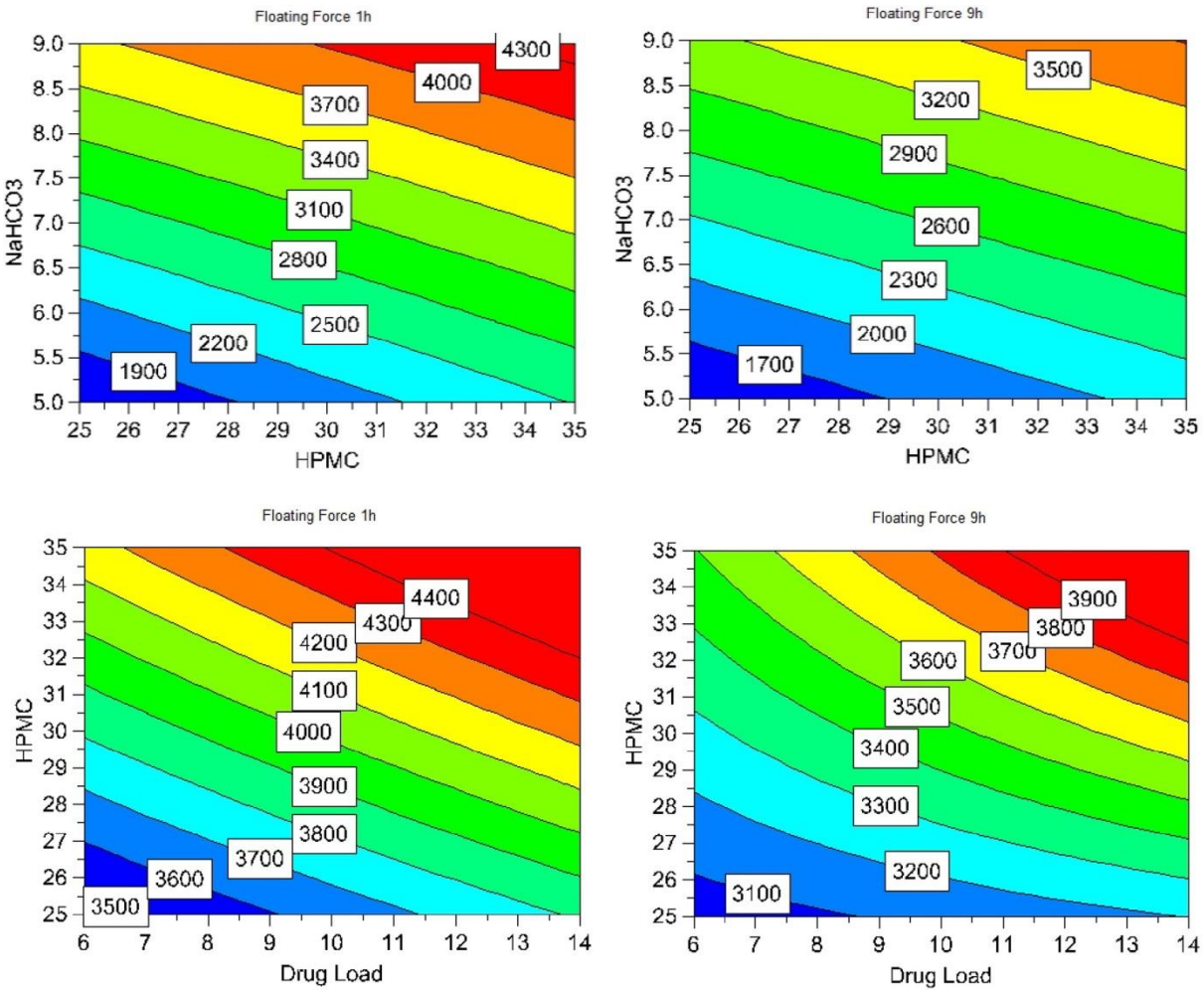

Fig. 8. Representative contours describing the effect of the variables on the floating strength of the pellets at (A) 1 h and (B) 9 h.

The stomach adhesion potential of the pellets was determined by measuring the bio-adhesion force. All 11 formulations were subjected to *ex vivo* bio-adhesion force measurement. The bio-adhesion force of a single measurement varied from 3.05–6.98 mN/pellet which was over three times larger than gravity of a saturated pellet, which ultimately weighed < 100 mg even at its heaviest. This could be inferred that every pellet could adhere well onto the stomach wall to prevent from being dislodged with gastric fluid during gastric emptying stage.

The average bio-adhesion force per pellets was in the range of 4.42 ± 1.53 mN to 5.67 ± 1.08 mN (Fig. 9). The differences in bio-adhesion force of the 11 formulations were not significant ($P = 0.875$, one-way ANOVA test using SPSS 22). There was no significant difference in the force between any two formulations ($P > 0.926$, Tukey test using SPSS 22). This might be explained by the fact that the chemical structure of HPMC and HPC, the two components that generate the adhesion force, are very similar. Therefore, the hydrogen bond intensity was not significantly affected by the HPMC/HPC ratio in the experimental range.

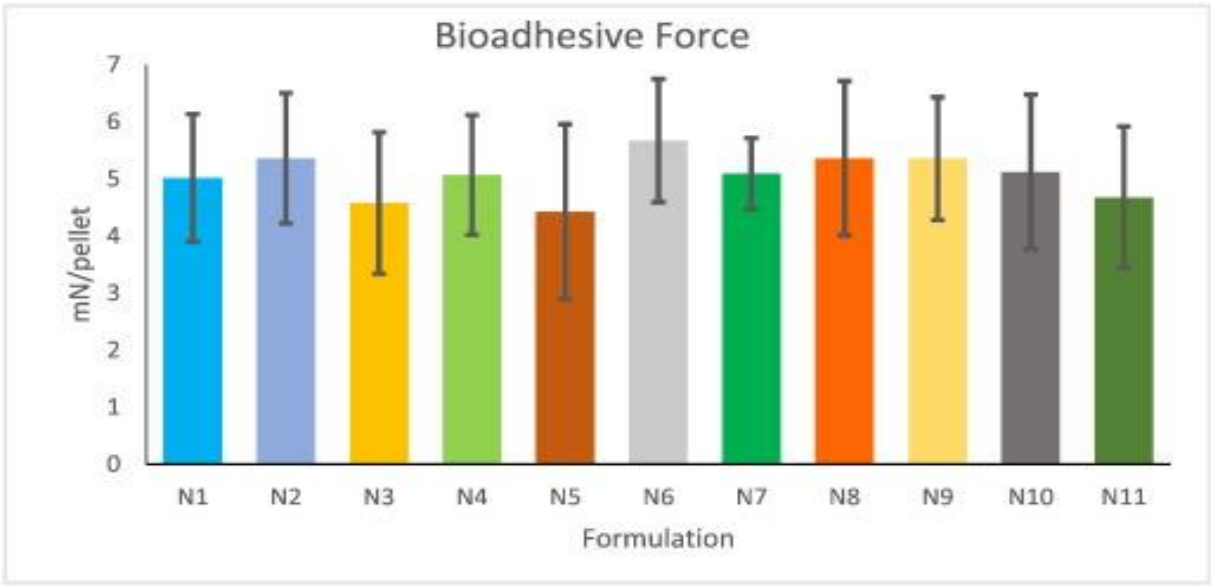

Fig-9: Average bio-adhesion force-per-pellet of the experimental formulations (± SD, *n* = 5).

More interestingly, the average bio-adhesion force was found to be relatively stable over the experimental time in the FaSSGF. This can be explained by the following: initially, when the outer polymer layer is not completely saturated, the hydrogel layer is highly viscous and dense, allowing the pellets to adhere more strongly to the stomach mucosa, but the size of the matrix is relatively small, so the contact area of a pellet to the mucosa is also small. Later on, the pellets are more saturated, and the gel layer became less adherent, but the matrix size is increased, so the contact area of the matrix to the mucosa is increased, thus maintaining the adhesion force. The matrix then proceeds into a steady state, in which the balance between the dissolution of polymer molecules at the matrix surface and the gelling of polymer molecules in the inner core is established, and the matrix size and the gel structure are stable enough to keep the adhesion force constant. The steady state was maintained up to 9 h before the polymer-dissolving process exceeded the polymer-gelling process, making the gel layer less adherent and decreasing the adhesion force.

The combination of floating and bio-adhesion has the potential to generate a synergistic effect that increases the probability of gastric retention. During the gastric emptying stage (phase 4 of the gastric physiology cycle), the contents of the stomach are pushed forward to the intestine along with gastric fluid; the pellets are expected to stay adhering to the stomach wall, thus ensuring that the pellets would not be pushed out and would remain in the stomach. However, if the pellets did detach from stomach wall because of the mucus shedding process, their buoyancy will keep them in the stomach. A new cycle of mucosal adhesion would start with a new mucosal layer. Therefore, this bio-adhesive floating DDS has high potential resistance to gastric biological activities, and is likely to remain in the stomach for a sufficient period of time.

3.5.Drug Release Kinetics:

In the Sink Condition

In the sink condition (SLS 1% in HCL 0.1 N, pH 1.2), drug release could be controlled up to 12 h. Even though dissolution was largely different between formulations, the pattern of the drug release profiles was very similar (Fig. 10) because the release mechanism was similar. HPMC and HPC rapidly swelled once the pellets contacted the gastric fluid, forming an outer gel layer (Fig. 5F). Drug molecules then diffused through the gel layer out to the dissolution medium. Knowing this, the thickness, denseness, and hydrophilicity of the gel layer would control the drug release kinetics. As can be seen from the results of the dissolution regression, drug load, SBC percentage, and HPMC content all affected drug release differently over the time. The average dissolution at 1, 3, 4, and 8 h (Table 4) was used to correlate the independent factors with dependent variables. From the regression results (Table 5), the three factors of drug load, SBC percentage, and HPMC content significantly affected drug dissolution at 1 h and 3 h ($P < 0.03$). The significance of the (HPMC content ∗ Drug load) and (SCB percentage ∗ Drug load) variables ($P < 0.05$) at 1 h indicate that there were interactions between these factors, meaning that the effect of one factor was dependent on the values of the others.

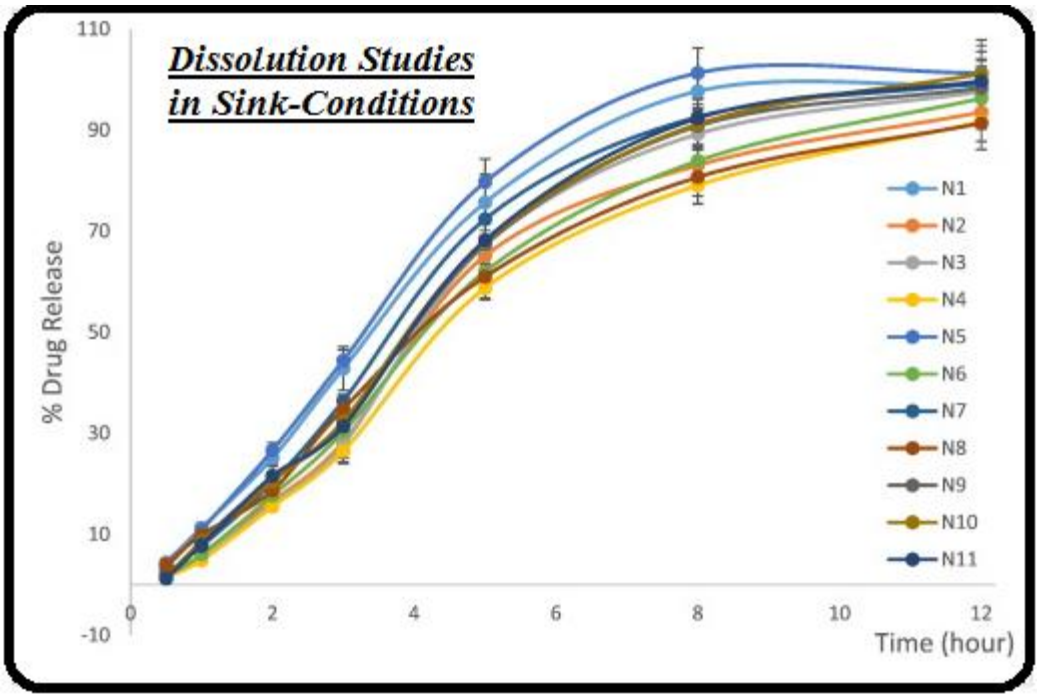

Fig.10: Dissolution profiles of experimental formulations in the sink condition (± SD, *n* = 3).

Table 6: Drug release kinetics.

Form.	Drug release (%)							
	1 h		3 h		5 h		8 h	
	Average	SD	Average	SD	Average	SD	Average	SD
N1	11.39	0.99	44.1	4.31	75.67	5.55	97.65	4.38
N2	5.33	0.59	28.5	3.29	65.2	4.21	83.17	3.42
N3	5.49	0.99	27.69	1.49	67.1	6.12	89.18	4.81
N4	4.89	0.4	26.49	2.58	58.9	2.42	79.23	3.59
N5	10.81	1.2	44.39	2.09	79.9	4.49	101.2	4.89
N6	6.1	0.7	30.2	5.88	62.1	2.91	84.02	6.84
N7	7.87	1.2	36.36	1.28	72.3	3.19	92.7	2.71
N8	9.19	2.2	34.76	1.58	60.99	4.21	80.3	5.42
N9	8.68	1.8	31.67	3.59	67.45	4.03	90.1	3.69
N10	8.59	0.49	32.84	3.08	67.89	4.26	91.4	4.87
N11	7.88	1.49	31.38	4.71	68.31	3.56	92.5	5.43

The dissolution profiles of 11 formulations and crude API in FaSSGF were shown in the Fig. 11. The dissolution profiles of all formulations were significantly different from that of the pure drug at all time points (P = 0.000, one-way ANOVA test). From 4 h onward, the drug concentration reached maximum values, which were not significantly different between all 11 formulations (P > 0.05, one-way ANOVA test). Drug release was slow during the first hour but increased from 1 to 4 h, before drug concentration peaked at approximately 2 µg/mL; this could be considered the drug's apparent solubility. From that time onward, the drug concentration was maintained relatively stable at its apparent solubility. In comparison, drug dissolution from the crude API was very slow, and its maximum concentration was 10 folds lower than that of the formulations.

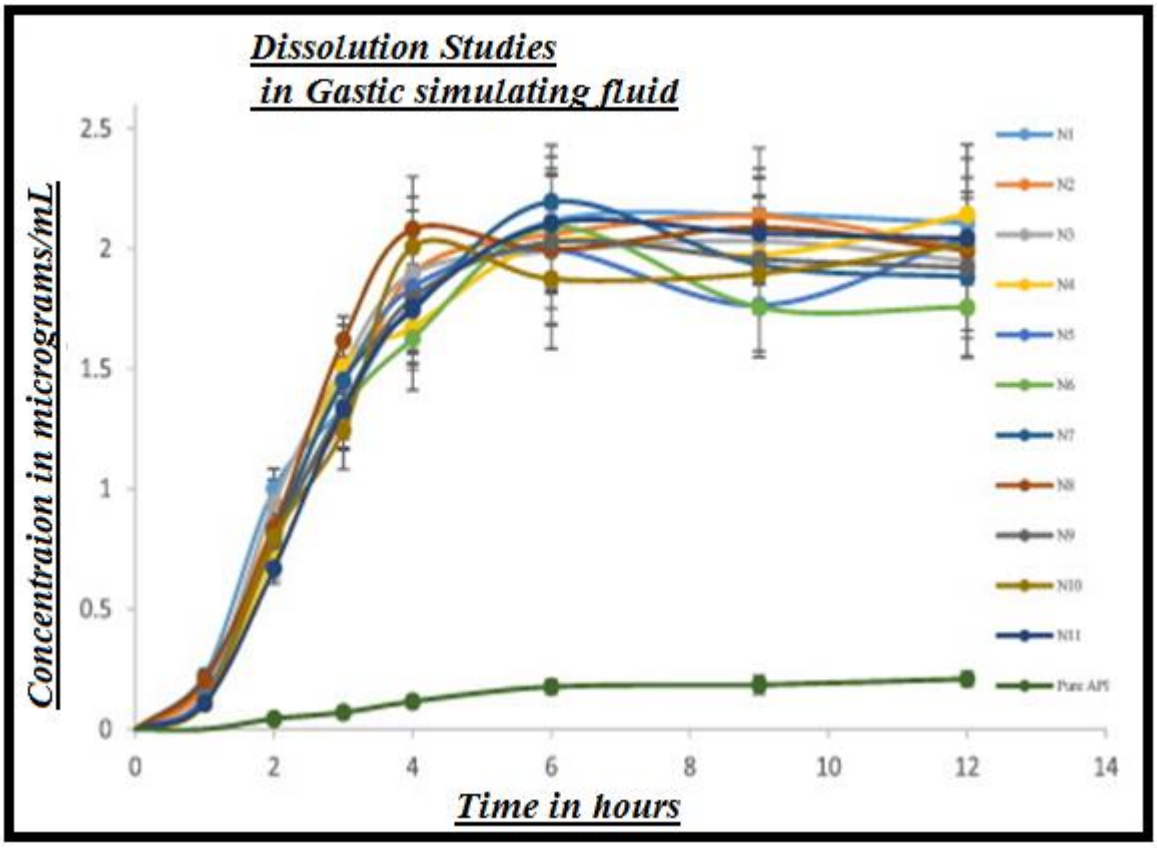

Fig. 11. Dissolution profiles of experimental formulations and crude API in FaSSGF (± SD, *n* = 3).

The regression results of various output variables can be utilized to design spaces for QBD. On the basis of the predetermined qualities of a finished product and the requirement range of various response variables, the properties of the finished product can be set. On a contour graph of each response variable, a satisfactory region where the response variable meets constraints can be determined. By overlaying all contours, an overlapping space will be generated by all the individual contour plots, called a "sweet spot" region. The "sweet spot" region can be considered a space in which processing parameters can vary without any change in product qualities. It can be considered equivalent to the design space concept of QBD, which is defined as ranges within which parameters can vary without considering as a change in process (Yu, 2008). For example, if the expected quality of the pellets were: 8% < Dissolution 1 h < 12%, 30% < Dissolution 3 h < 45%, 45% < Dissolution 5 h < 70%, Dissolution 8 h > 80%, floating force at 1 h > 2500 μN/g, and floating force at 9 h > 2500 μN/g, then the sweet spots would be generated as the red area in the plot at the level of A) 6%, B) 10%, and C) 14% drug load (Fig.12). Each point on the plot represents a paired value for HPMC content and SBC percentage. If a representative point changes within the sweet spot area, the setting constraints are still satisfied. Applying this principle in production, compositions might vary because of random or systematic errors, but variable limits should be determined to ensure that formula compositions do not fall out of the "sweet spot" area.

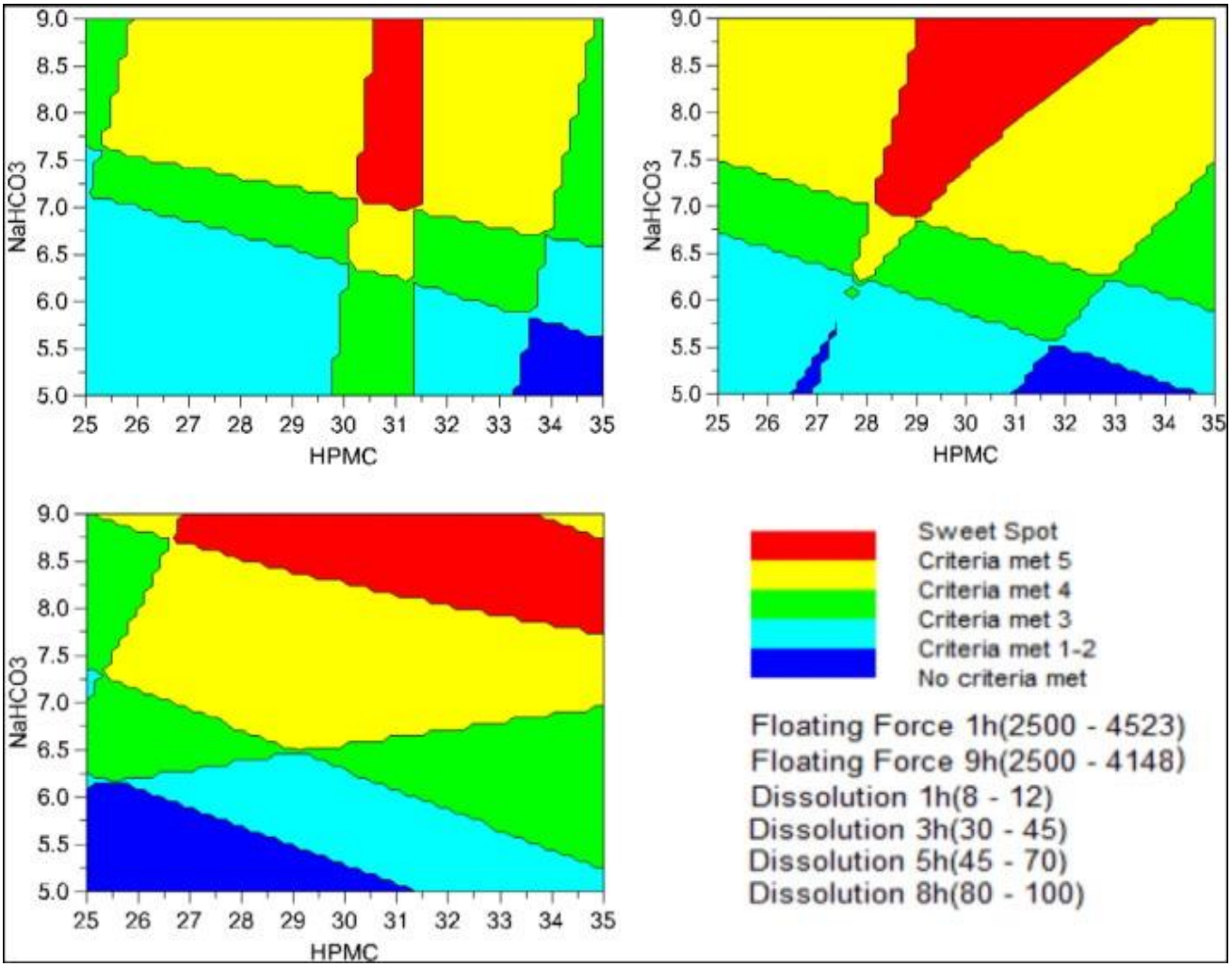

Fig.-12**: Illustration of sweet-spot application in QBD design space. A) Low drug load. (B) Medium drug load. (C) High drug load. (D) Constrained criteria.**

CONCLUSION:

Bio-adhesive floating pellets loaded with amorphous SD were successfully fabricated using HME technology. The results of this study showed that the pellets can be utilized as a platform for manufacturing a viable gastro-retentive controlled-release DDS. The pellets were well characterized, and the effects of various factors on pellet properties were regressively correlated. The pellets had excellent bio-adhesion, a high and stable floating force, and a capability for controlled drug release up to 12 h. The dual gastro-retentive mechanisms of the pellets are highly resistant to stomach physiological activities, which tend to push dosage forms out of the stomach into the intestine. The FEL amorphous SD generated *in situ* super-saturation that would ultimately help the drug absorb more consistently and completely. This study has the potential to systematically scale up by applying the design space QBD concept.

REFERENCES:

1. Chen, R.N., Ho, H.O., Yu, C.Y., Sheu, M.T., 2010. Development of swelling/floating gastro-retentive drug delivery system based on a combination of hydroxyethyl cellulose and sodium carboxymethyl cellulose for losartan and its clinical relevance in healthy volunteers with CYP2C9 polymorphism. Eur. J. Pharm. Sci. 39, 82–89.

2. Forster, A., Hempenstall, J., Tucker, I., Rades, T., 2001. The potential of small-scale fusion experiments and the Gordon-Taylor equation to predict the suitability of drug/polymer blends for melt extrusion. Drug Dev. Ind. Pharm. 27, 549–560.

3. Fukuda, M., Peppas, N.A., McGinity, J.W., 2006. Floating hot-melt extruded tablets for gastro-retentive controlled drug release system. J. Control. Release 115, 121–129.

4. Islam, M.T., Scoutaris, N., Maniruzzaman, M., Moradiya, H.G., Halsey, S.A., Bradley, M.S., Chowdhry, B.Z., Snowden, M.J., Douroumis, D., 2015. Implementation of transmission NIR as a PAT tool for monitoring drug transformation during HME processing. Eur. J. Pharm. Biopharm. 96, 106–116.
5. Konno, H., Handa, T., Alonzo, D.E., Taylor, L.S., 2008. Effect of polymer type on the dissolution profile of amorphous solid dispersions containing felodipine. Eur. J. Pharm. Biopharm. 70, 493–499.
6. Lopes, C.M., Bettencourt, C., Rossi, A., Buttini, F., Barata, P., 2016. Overview on Gastro-reentive drug delivery systems for improving drug bioavailability. Int. J. Pharm.
7. Malode, V.N., Paradkar, A., Devarajan, P.V., 2015. Controlled release floating multiparticulates of metoprolol succinate by hot melt extrusion. Int. J. Phar. 491, 345–351.
8. Marques, M.R.C., Liebenberg, R., Almukainzi, M., 2011. Simulated biological fluids with possible application in dissolution testing. Dissolut. Technol. 18, 15–28.
9. Newton, J.M., 2010. Gastric emptying of multi-particulate dosage forms. Int. J. Pharm. 395, 2–8.
10. Pawar, V.K., Kansal, S., Asthana, S., Chourasia, M.K., 2012. Industrial perspective of gastro-retentive drug delivery systems: physicochemical, biopharmaceutical, technological and regulatory consideration. Expert Opin. Drug Deliv. 9, 551–565.
11. Podczeck, F., 2010. Gastrointestinal transit and functionality of multiple unit dosage forms. Int. J. Pharm. 395, 1.
12. Repka, M.A., Battu, S.K., Upadhye, S.B., Thumma, S., Crowley, M.M., Zhang, F., Martin, C., McGinity, J.W., 2007. Pharmaceutical applications of hot-melt extrusion: part II. Drug Dev. Ind. Pharm. 33, 1043–1057.
13. Repka, M.A., Majumdar, S., Kumar Battu, S., Srirangam, R., Upadhye, S.B., 2008. Applications of hot-melt extrusion for drug delivery. Expert Opin. Drug Deliv. 5, 1357–1376.
14. Rouge, N., Buri, P., Doelker, E., 1996. Drug absorption sites in the gastrointestinal tract and dosage forms for site-specific delivery. Int. J. Pharm. 136, 117–139.
15. Sarode, A.L., Sandhu, H., Shah, N., Malick,W., Zia, H., 2013. Hot melt extrusion (HME) for amorphous solid dispersions: predictive tools for processing and impact of drugpolymer interactions on super-saturation. Eur. J. Pharm. Sci. 48, 371–384.
16. Siepmann, J., Peppas, N., 2001. Modeling of drug release from delivery systems based on hydroxypropyl methylcellulose (HPMC). Adv. Drug Deliv. Rev. 48, 139–157.
17. Singh, B.N., Kim, K.H., 2000. Floating drug delivery systems: an approach to oral controlled drug delivery via gastric retention. J. Control. Release 63, 235–259.
18. Streubel, A., Siepmann, J., Bodmeier, R., 2006. Drug delivery to the upper small intestine window using gastro-retentive technologies. Curr. Opin. Pharmacol. 6, 501–508.
19. Taupitz, T., Dressman, J.B., Klein, S., 2013. In vitro tools for evaluating novel dosage forms of poorly soluble, weakly basic drugs: case example ketoconazole. J. Pharm. Sci. 102, 3645–3652.
20. Tumuluri, V.S., Kemper, M.S., Lewis, I.R., Prodduturi, S., Majumdar, S., Avery, B.A., Repka, M.A., 2008. Off-line and on-line measurements of drug-loaded hot-melt extruded films using Raman spectroscopy. Int. J. Pharm. 357, 77–84.
21. Van Den Abeele, J., Rubbens, J., Brouwers, J., Augustijns, P., 2016. The dynamic gastric environment and its impact on drug and formulation behaviour. Eur. J. Pharm. Sci. 96, 207–231.
22. Varum, F.J., Veiga, F., Sousa, J.S., Basit, A.W., 2010. An investigation into the role of mucus thickness on mucoadhesion in the gastrointestinal tract of pig. Eur. J. Pharm. Sci. 40, 335–341.
23. Vasconcelos, T., Sarmento, B., Costa, P., 2007. Solid dispersions as strategy to improve oral bioavailability of poor water soluble drugs. Drug Discov. Today 12, 1068–1075.
24. Vo, A.Q., Feng, X., Morott, J.T., Pimparade, M.B., Tiwari, R.V., Zhang, F., Repka, M.A., 2016. A novel floating controlled release drug delivery system prepared by hot-melt extrusion. Eur. J. Pharm. Biopharm. 98, 108–121.
25. Wahl, P.R., Treffer, D.,Mohr, S., Roblegg, E., Koscher, G., Khinast, J.G., 2013. Inline monitoring and a PAT strategy for pharmaceutical hot melt extrusion. Int. J. Pharm. 455, 159–168.
26. Yang, X., Shen, B., Huang, Y., 2015. Mechanistic study of HPMC-prolonged super-saturation of hydrocortisone. Cryst. Growth Des. 15, 546–551.
27. Yu, L.X., 2008. Pharmaceutical quality by design: product and process development, understanding, and control. Pharm. Res. 25, 781–791.